

Characteristics of Desertification Change in Lake Basin Area in Gangcha County

Wenzheng Yu¹, Mingxuan Zhu¹, Li Shao¹, Yanbo Shen^{2,3,*}, Haitao Liu¹, Tianliang Chen¹ and Hanxiaoya Zhang⁴

¹School of Geographical Sciences, Nanjing University of Information Science & Technology, Nanjing, 210044, China

²Public Meteorological Service Center, China Meteorological Administration, Beijing, 100081, China

³Center for Wind and Solar Energy Resources, China Meteorological Administration, Beijing, 100081, China

⁴Faculty of Science, The University of Auckland, Auckland, 1010, New Zealand

*Corresponding Author: Yanbo Shen. Email: shenyb@cma.gov.cn

Received: 10 January 2022; Accepted: 23 March 2022

Abstract: Qinghai Lake Basin area in Gangcha county is selected as the study area in terms of desertification change features in this paper. Based on the remote sensing (RS) and global positioning system (GPS) technologies, the desertification information range from 1989 to 2014 in the study area is extracted. Using the method of the decision tree, the desertification in the research area is been divided into four grades including mild desertification, moderate desertification, severe desertification and serious desertification. The change characteristics of desertification in the study area were analyzed in detail, which showed that the desertification in the study area experienced a process of first development and then a reversal. The rapid development of desertification appears in the 1990s, where about 1101.22 kilometers of desertification area was increased in this stage. Since the twenty-first Century, the desertification is gradually significant recovered and local area exist intensified desertification. There are tendencies of interactive transform in different types of desertification. The tendencies of different degrees of desertification land are rising, and there're some differences in rising rates, where the expansion rate of moderate desertification is the biggest, increasing by 7.27 kilometers per year.

Keywords: Desertification classification; desertification expansion rate; grass land change; the Qinghai Lake

1 Introduction

Desertification is a manifestation of land degradation, which was first proposed by Lavauden [1]. However, the definitions of desertification are still not reached a consensus [2]. It was not until 1999 that the definition of desertification was widely applied in academic circles in the United Nations Convention to Combat Desertification, which pointed out that desertification is the land degradation



This work is licensed under a Creative Commons Attribution 4.0 International License, which permits unrestricted use, distribution, and reproduction in any medium, provided the original work is properly cited.

in arid, semi-arid, and semi-humid areas caused by a variety of factors including climate change and human activities [3]. Desertification, threatened human survival and sustainable development, has become one of the most serious ecological environment and social-economic problems.

Desertification mapping is the important and fundamental work for studies of the mechanism of desertification, spatial and temporal change of land degradation. Hanan et al. [4] used remote sensing data to evaluate the desertification in the Sahara desert. Tripathy et al. [5] extracted Albedo, normalized difference vegetation index (NDVI), land erosion rate and, soil moisture from Multispectral Scanner (MSS) images to evaluate land degradation in the Karnataka region of India by selecting. Nasem et al. [6] used temporal and spatial dynamic index of vegetation coverage to dynamically monitor desertification change in Egypt through multi-temporal moderate-resolution imaging like spectroradiometer (MODIS) remote sensing data. Wu [7,8] proposed a series of remote sensing dynamic monitoring methods based on the technical route of discriminant indicators and monitoring of desertified land; then, the authors found that the desertified land change in the Horqin region experienced a process of development-redevelopment-reversal in recent 50 years. Based on remote sensing images, Li et al. [9] believed through discussion and analysis that desertification in the Otindag Sandy Land would develop further in the 21st century under the background of global warming. Hu et al. [10,11] monitored desertification in the source region of the Yellow River in recent 30 years by combining remote sensing and geographic information system technology and found that the area of desertified land in the source region of the Yellow River showed an increasing trend, and further verified and analyzed the development of desertification combining landscape pattern analysis. For the study of desertification in China, many scholars mainly put their efforts into the typical sandy land in north China (Horqin Sandy Land, Mu Us Sandy Land, Otindag Sandy Land, Hulun Buir Sandy Land, etc.), ecologically fragile river source regions and the Qinghai-Tibet Plateau [12,13]. These studies have analyzed the dynamic changes of desertification in these regions, but the driving mechanism of desertification is mostly discussed by qualitative methods, and the screening of main controlling factors of desertification is lacking.

The sensitivity of desertification in the surrounding area of the Qinghai Lake is moderate and high. In recent years, the desertification situation in the Qinghai Lake area has been quite serious. Therefore, the Qinghai Lake area has become one of the hot spots and focus areas of desertification around the world. Therefore, Gangcha County was selected as a representative county to carry out relevant research and provide scientific decision-making basis for desertification prevention and control.

The remainder of this paper is organized as follows. Section 2 describes the study area. Section 3 describes the data preprocessing. Then, Section 4 describes the research methods. Next, Section 5 demonstrates and discusses the research results in detail, and finally, Section 6 presents the conclusions.

2 Study Area

Study area, on the north bank of Qinghai Lake, is located at Gangcha County, Haibei Tibetan Autonomous Prefecture, Qinghai Province. The geographical location is between $99^{\circ}20'44''$ – $100^{\circ}37'24''$ E, $36^{\circ}58'06''$ – $38^{\circ}04'04''$ N, bordering Haiyan County on the east, Tianjun County of Haixi Mongolian and Tibetan Autonomous Prefecture on the west, Buha River and Hainan County on the south, and Tonghe River on the north. The total area is 1.2×10^4 km², and the land type is mainly grassland. The terrain of the study area is clear north high and south low, with an average altitude of more than 3300 m. Gangcha county is a typical highland continental climate, long sunshine time, the large temperature difference between day and night; The average annual precipitation is 370.5 mm, and the annual evaporation is 1500.6~1847.8 mm. It is cool in summer and autumn and cold in winter. The

average annual temperature is only -0.6°C . In this paper, the southern lake basin area with obvious desertification development was selected as the research area (As shown in Fig. 1).

Lake Basin Area of Gangcha County



Figure 1: Image of the study area

3 Data Preprocessing

This paper mainly uses Landsat 5 Thematic Mapper (TM) remote sensing image data to interpret and obtain the land cover in the study area. Landsat data is obtained by NASA, which is favored for its advantages of multi-band, good spatial resolution (30 M) and short monitoring period, especially its superior potential in long-term continuous remote sensing monitoring at the large regional scale. In this study, Landsat 5 TM images from 1989 to 2014 were selected as the main data source. The images were mainly taken from July to September when the vegetation coverage of the Gangcha Lake basin area was better and the thermal radiation difference of ground objects was more obvious, and the cloud content of the images was less than 10%. Specific image information is shown in Tab. 1.

Table 1: Remote sensing data

Serial number	Type of data	Imaging time	Track number	Number of bands	Spatial resolution (m)
1	Landsat5 TM	1989.08	p133r34	7	30.0
2	Landsat5 TM	1990.06	p133r34	7	30.0
3	Landsat5 TM	1993.08	p133r34	7	28.5
4	Landsat5 TM	1995.08	p133r34	7	30.0
5	Landsat5 TM	1996.06	p133r34	7	28.5
6	Landsat5 TM	1997.08	p133r34	7	28.5
7	Landsat5 TM	1998.07	p133r34	7	28.5
8	Landsat5 TM	1999.07	p133r34	7	28.5
9	Landsat5 TM	2000.08	p133r34	7	30.0
10	Landsat5 TM	2001.07	p133r34	7	30.0
11	Landsat5 TM	2002.07	p133r34	7	30.0

(Continued)

Table 1: Continued

Serial number	Type of data	Imaging time	Track number	Number of bands	Spatial resolution (m)
12	Landsat5 TM	2003.09	p133r34	7	30.0
13	Landsat5 TM	2004.09	p133r34	7	30.0
14	Landsat5 TM	2005.09	p133r34	7	30.0
15	Landsat5 TM	2006.08	p133r34	7	30.0
16	Landsat5 TM	2008.07	p133r34	7	30.0
17	Landsat5 TM	2009.08	p133r34	7	30.0
18	Landsat5 TM	2010.07	p133r34	7	30.0
19	Landsat5 TM	2011.06	p133r34	7	30.0
20	Landsat8 OLI	2013.09	p133r34	11	30.0
21	Landsat8 OLI	2014.07	p133r34	11	30.0

Due to attenuation and satellite flight attitude sensor function, the effect of many factors, such as atmosphere and at the time of complex surface information, will inevitably produce a variety of radiation distortion, geometric distortion and atmospheric extinction system error and random error, which is to reduce the quality of the remote sensing image and affects the accuracy of image analysis [14]. Therefore, it is necessary to preprocess remote sensing images. In this study, remote sensing image preprocessing includes radiometric calibration, atmospheric correction, geometric correction, image clipping, etc. All preprocessing operations are based on the environment for visualizing images (ENVI) 5.0 platform.

4 The Research Methods

4.1 Selection and Inversion of Desertification Monitoring Index

On the basis of the interpretation of the desertification results, the desertification vector diagrams of 1990 and 2000, 2000 and 2009, and 2009 and 2014 were superimposed and calculated, obtained the years 1990 to 2000, 2000 to 2009, and the transfer matrix of various types of desertified land in the three periods, and analyzed the evolution mechanism of different types of desertified land in two different time dimensions: interdecadal and interannual.

4.1.1 Albedo

Albedo refers to the ratio of solar radiation reflected by the earth's surface, that is, the ratio of the solar radiation flux reflected by the Earth's surface to the solar radiation flux incident. Surface Albedo, or surface Albedo, reflects the earth's ability to reflect solar radiation. Radiation from the sun drives the land, sea, air the material exchange and energy cycle of the ecosystem, absorbed by the surface solar radiation conditions but also will affect the entire earth's weather and climate change. So the surface albedo is the key factor of the development and changes of the earth's climate system, it is an important parameter of the terrestrial surface radiation energy balance. Referring to the calculation method, this study uses the reflectance in the direction of the top of the atmosphere to estimate the surface albedo of the wideband, and the calculation formula is as follows:

$$\text{Albedo} = 0.356R_1 + 0.130R_3 + 0.373R_4 + 0.085R_5 + 0.072R_7 - 0.0018 \quad (1)$$

where, R_1, R_3, R_4, R_5, R_7 are the first, third, fourth, fifth and seventh bands of TM image respectively.

4.1.2 Vegetation Coverage

Fractional Vegetation Cover (FVC) refers to the vertical projection area of Vegetation in the unit area [15], which is one of the important input parameters in land desertification evaluation, soil erosion monitoring and ecological environment assessment [16]. Vegetation coverage is usually estimated using NDVI. NDVI is a comprehensive reflection of vegetation type cover form and growth status within a unit pixel [16]. Its characteristics are mainly shown as follows: When the pixel is completely covered by vegetation, the corresponding NDVI value is 1; when there is no vegetation coverage at all, the corresponding NDVI value is between -1 and 0 , such as water body and desert; when vegetation cannot completely cover the whole pixel, the corresponding NDVI value is between 0 and 1 , and such pixel is called a mixed pixel. The calculation formula of normalized vegetation index NDVI is as follows:

$$\text{NDVI} = (NIR - R) / (NIR + R) \quad (2)$$

where NIR and R are the near-infrared band and red band of the image respectively.

According to the binary pixel model [17,18], the estimation formula of vegetation coverage is as follows:

$$Fc = (ndvi - ndvi_{soil}) / (ndvi_{veg} - ndvi_{soil}) \quad (3)$$

In the formula, $ndvi_{soil}$ is the NDVI value of the area without vegetation coverage, and $ndvi_{veg}$ is the NDVI value of the area completely covered by vegetation. Due to the influence of solar radiation, the values of $ndvi_{soil}$ and $ndvi_{veg}$ are different from 0 and 1 . Normally, the range of $ndvi_{soil}$ varies from -0.1 to 0.2 , and the range of $ndvi_{veg}$ varies from 0.6 to 0.8 .

4.1.3 Modified Soil Adjusted Vegetation Index

To reduce the influence of soil, shadow, atmospheric environment and other factors on the vegetation index inversion results, the improved soil-adjusted vegetation index (MSAVI) came into being. MSAVI can minimize the influence of soil factors and enhance sensitivity to vegetation [19]. As an important indicator of desertification classification, MSAVI can not only eliminate the influence of soil factors but also obtain objective results without artificial parameters. The specific calculation formula is as follows:

$$\text{MSAVI} = \left(2NIR + 1 - \sqrt{(2NIR + 1)^2 - 8(NIR - R)/2} \right) \quad (4)$$

where NIR and R are the near-infrared band and red band of the image respectively.

4.1.4 Land Surface Temperature

Land Surface Temperature (LST), which is an important parameter in desertification monitoring, will change with the change of desertified Land types. Land surface temperature inversion is mainly based on remote sensing data with the thermal infrared band. At present, LST inversion algorithms mainly include atmospheric correction method, single-channel algorithm, split window algorithm, and multi-band algorithm. In this study, the single-channel algorithm proposed by Weng Qihao et al. was used to invert land surface temperature.

First, the gray value is converted into the emitted radiation energy of the object, and the formula is as follows:

$$L_\lambda = a \times \text{DN} + b \quad (5)$$

Where, L_λ is the emitted radiation energy of each pixel in the thermal infrared band, and the unit is $\text{W}/(\text{m}^2 \cdot \text{sr} \cdot \mu\text{m})$; a is the gain coefficient, b is the offset coefficient. For Landsat5 TM image data, a value is 0.005631, b value is 0.124.

Secondly, the radiation energy emitted by the object is converted into the brightness temperature of surface radiation, and the transformation formula is as follows:

$$T_B = \frac{K_2}{\ln\left(\frac{K_1}{L_\lambda} + 1\right)} \quad (6)$$

Where, T_B is the brightness temperature of each pixel, in the unit of K; K_1 and K_2 are constants. In Landsat5 TM images, the value of K_1 is $607.76 \text{ mW}/(\text{cm} \cdot \text{sr} \cdot \mu\text{m})$, and the value of K_2 is 1260.56 K.

Then, the brightness temperature can be converted to the surface temperature, and the calculation formula is as follows:

$$T_s = \frac{T_B}{1 + (\lambda \times T_B / \rho) \ln \varepsilon} \quad (7)$$

$$\rho = hc/\alpha \quad (8)$$

Where, $\lambda = 11.5 \mu\text{m}$; h is Planck constant, 6.26×10^{-34} , unit is J·S; c is the speed of light, and the value is $2.998 \times 10^8 \text{ m/s}$. α is Stefan Boltzmann constant, with a value of 1.38×10^{-23} , and the unit is J/K. ε is the specific emissivity. The modified specific emissivity method proposed by Qin [20] is adopted for correction, and the formula is as follows:

$$\varepsilon = P_v R_v \varepsilon_v + (1 - P_v) R_s \varepsilon_s + d_\varepsilon \quad (9)$$

In the formula, P_v is vegetation coverage, R_v and R_s are temperature ratios of pure vegetation and pure bare soil respectively, ε_v and ε_s are specific emissivity of pure vegetation and pure bare soil respectively, and d_ε is a geometric shape. In the case of the relatively flat surface, d_ε is generally 0.

4.1.5 Soil Moisture

Soil moisture (WET) is an important indicator for monitoring land degradation and is of great significance for remote sensing monitoring and quantitative evaluation of desertification. The vegetation canopy temperature is affected by soil moisture. Sandholt et al. [21] found in their study that there were many isolines in the feature spatial distribution of TS-NDVI, so they proposed the concept of temperature vegetation drought index (TVDI). TVDI is calculated by land surface temperature and vegetation index, and the specific calculation formula is as follows:

$$\text{TVDI} = \frac{T_s - (a_2 + b_2 * \text{NDVI})}{(a_1 + b_1 * \text{NDVI}) - (a_2 + b_2 * \text{NDVI})} \quad (10)$$

where T_s is land surface temperature; a_1 , b_1 are the fitting dry-side equation coefficients; a_2 and b_2 are the coefficients of fitting the wet boundary equation. NDVI is the normalized vegetation index.

4.2 Extraction of Desertification Information In The Study Area

Remote sensing image classification is the prerequisite to evaluate the degree and spatial distribution of land desertification in the study area. The nature of decision tree classification is a kind of supervised classification, and its classification steps can be roughly divided into the following steps: First, the definition of knowledge (rules), which can be expressed by mathematical language such as algorithm, or defined by experience summary; Second is the input of rules, that is, the defined classification rules are input to the classifier; Thirdly the decision tree operation is carried out; Finally, the classification results are processed after output. Before decision tree classification, it is necessary to fuse the inverted vegetation coverage, albedo, land surface temperature, improved soil-adjusted vegetation index, and soil moisture image to obtain a new multi-band remote sensing image, which is used as the input layer of decision tree classification. In order to refine the desertification grade of the study area, the desertification grade of the study area was divided into seven categories: mild desertification, moderate desertification, severe desertification, severe desertification, non-desertification land, water body, and others (including cloud, cloud shadow, and snow).

According to the mathematical statistics of inversion parameters, the classification thresholds of desertification degree of different grades were set. In general, NDVI value can distinguish the vegetation covered area from the non-vegetation covered area, and the vegetation coverage can effectively distinguish the mild desertification land, moderate desertification land, severe desertification land, and desertified land. Albedo can efficiently cloud, the cloud and snow from vegetation types in the land to the isolated, the surface temperature can distinguish between water and serious desertification land types, the modified soil adjusted vegetation index and soil moisture can further distinguish between vegetation and vegetation coverage less desertification, water, and different land types such as cloud. The specific classification rules of the decision tree are shown in Fig. 2.

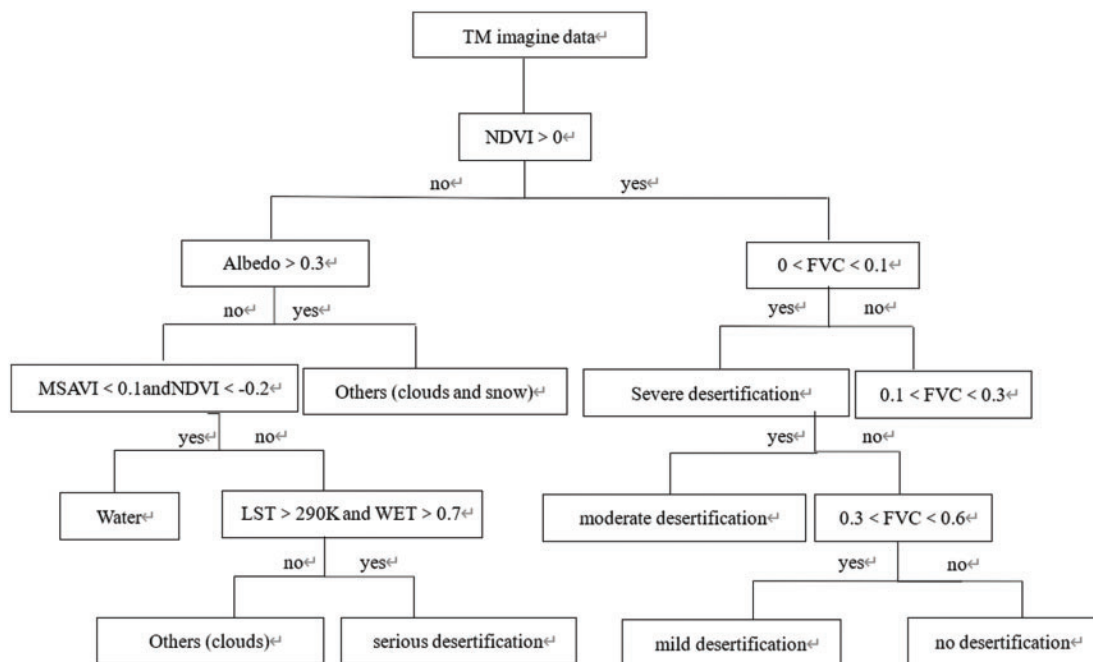


Figure 2: Decision tree classification rules

Established based on the decision tree classification system of land desertification in the study area can be divided into different levels, classification of inevitably in the salt and pepper effect, this is caused by noise classification error, the classification results are on ENVI 5.0 platform post-processing to remove salt and pepper effect to get the final results of desertification hierarchy, as shown in Fig. 3. In this study, the Error Matrix method was adopted to calculate the overall classification accuracy, Kappa coefficient, user classification accuracy, producer classification accuracy, and other indicators [22]. The overall classification accuracy of the calculated classification results was about 89%. The Kappa coefficients obtained are all greater than the minimum allowable discrimination accuracy of 0.7 [23], and the values are all above 0.8, which meet the accuracy requirements of remote sensing image classification [24–28].

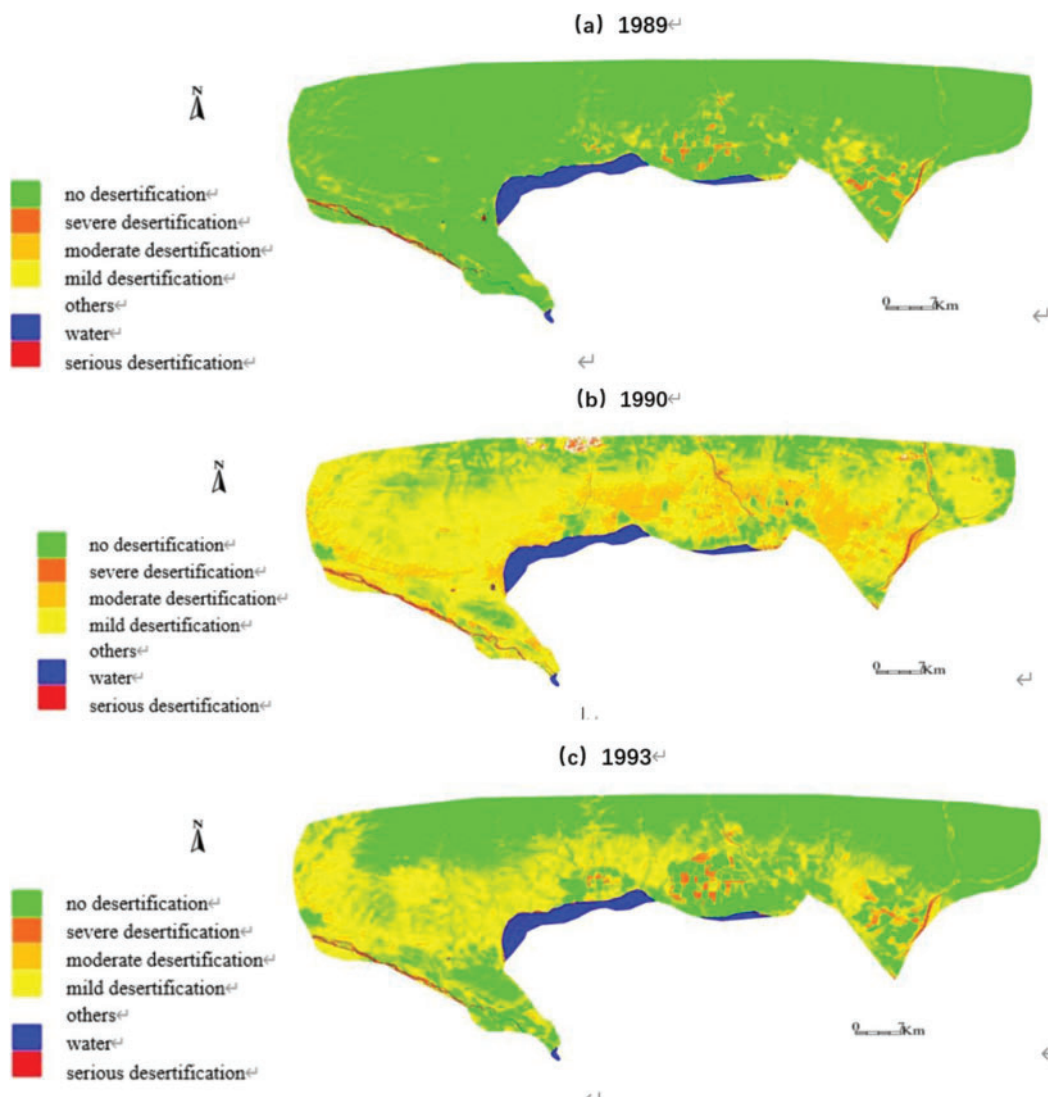


Figure 3: (Continued)

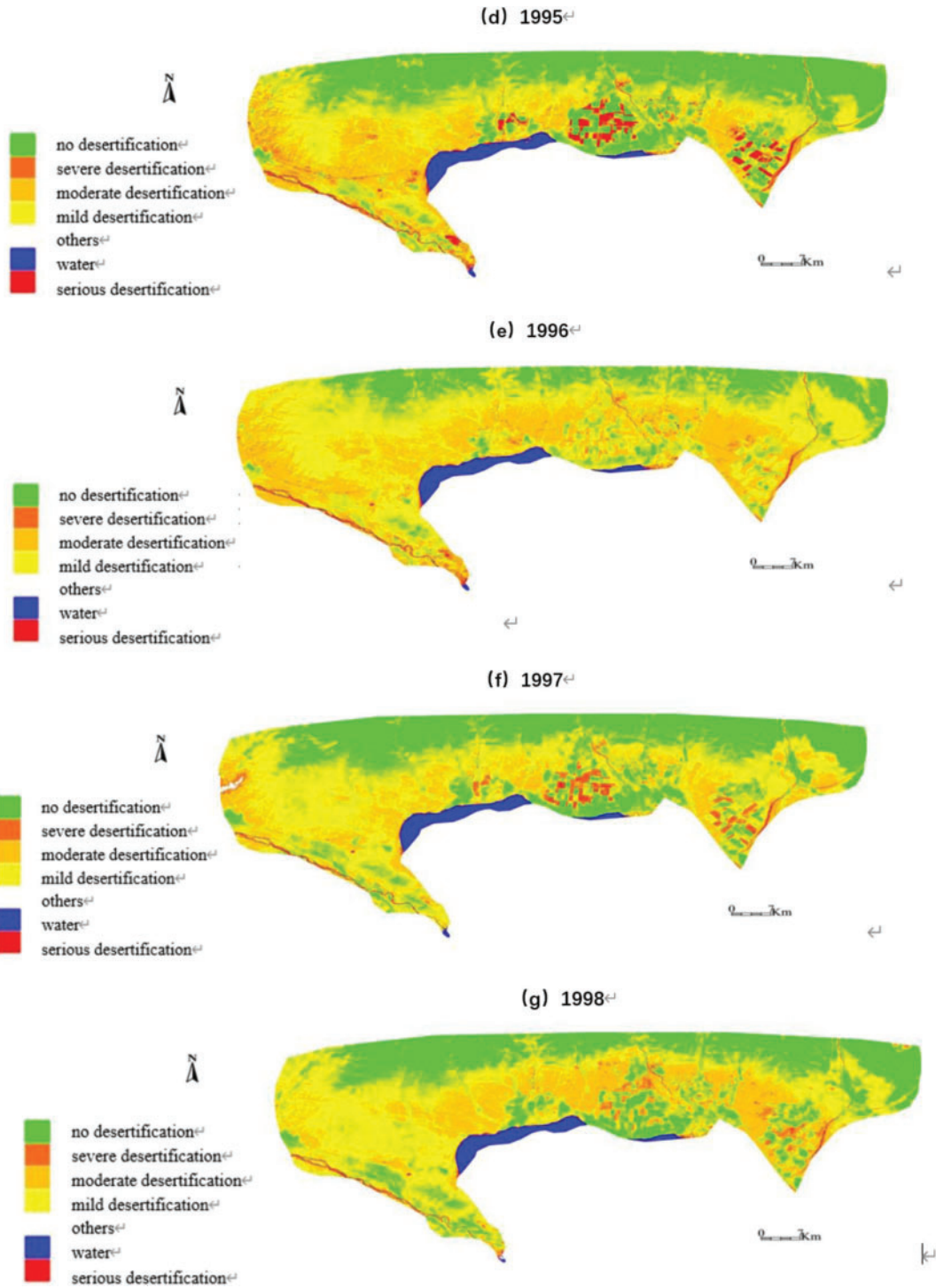


Figure 3: (Continued)

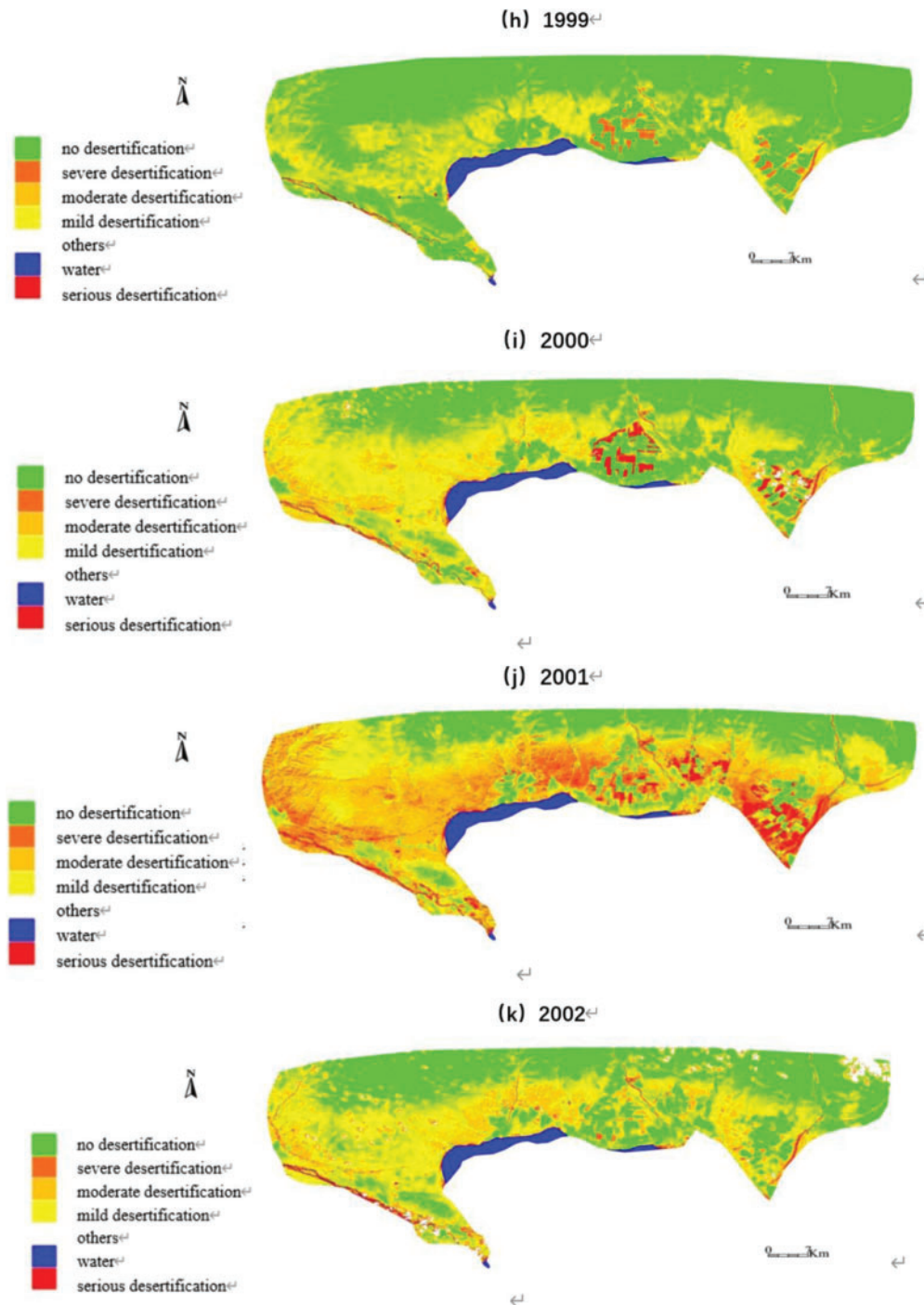


Figure 3: (Continued)

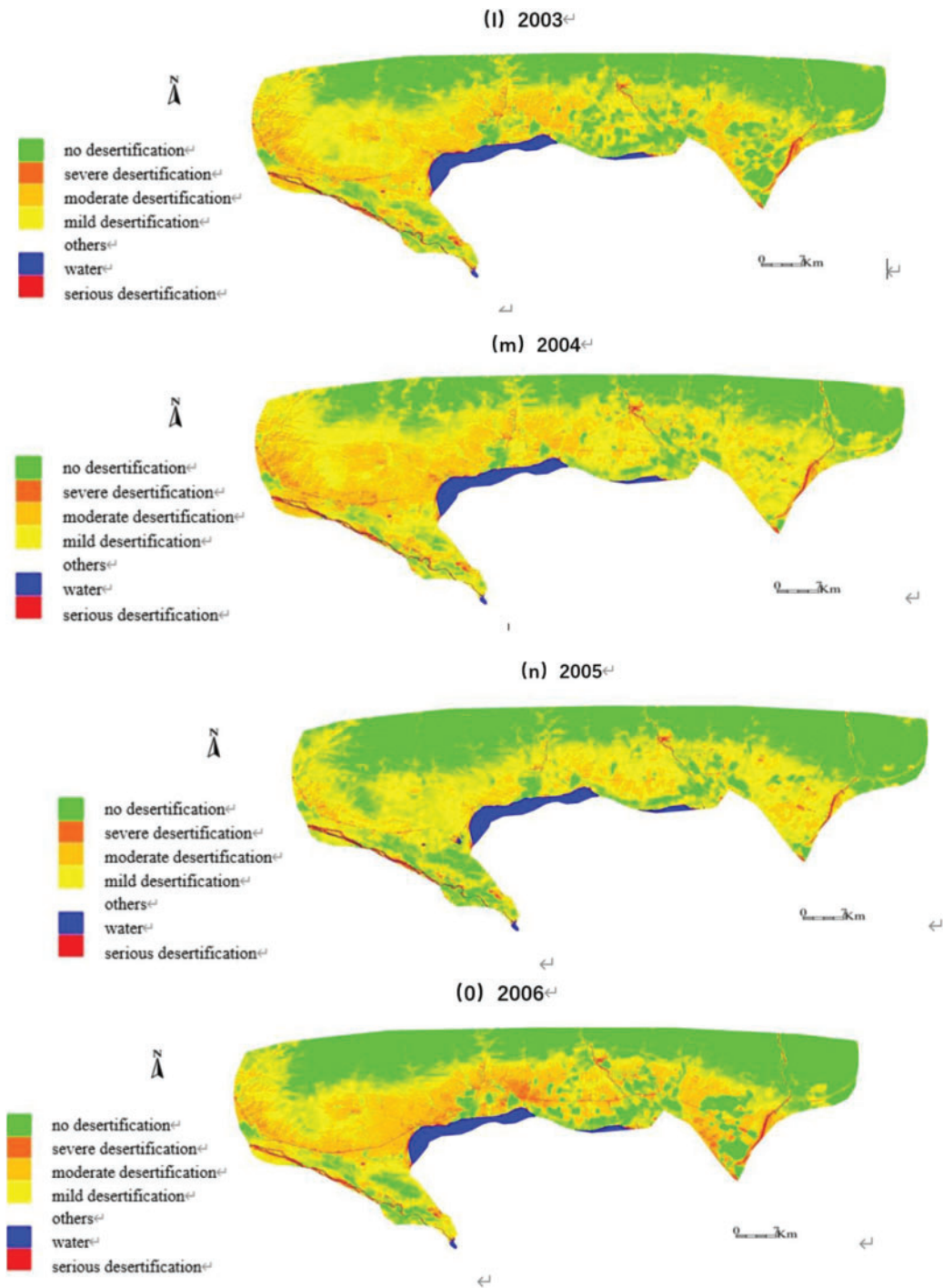


Figure 3: (Continued)

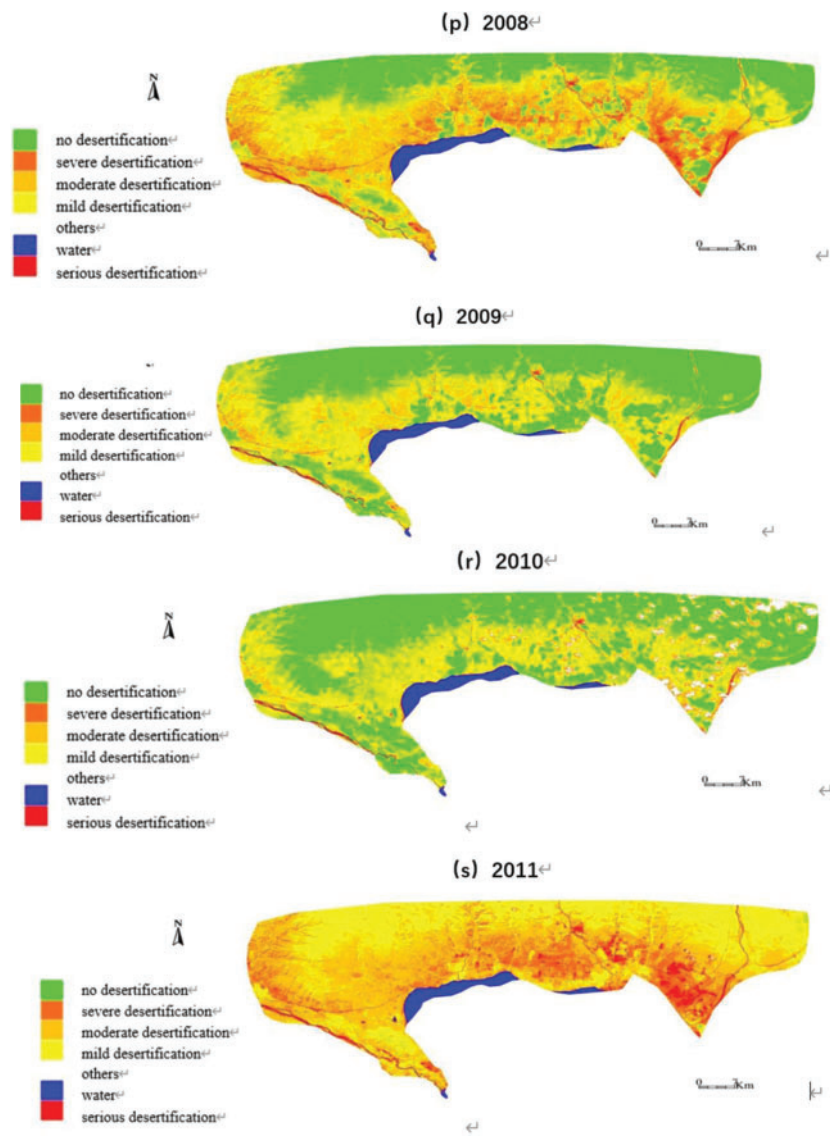


Figure 3: (Continued)

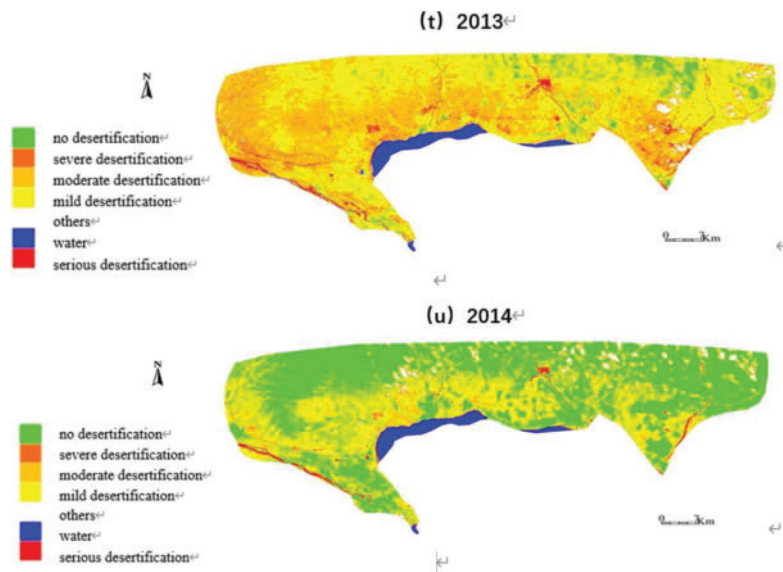


Figure 3: Land classification map of the study area in different periods

5 Change of Desertified Land In The Study Area

5.1 Interannual Variation of Desertified Land Area

Taking 1989, 2000, 2009, and 2014 as the time nodes, the research period was divided into three stages, and the area information of desertified land in different time nodes and periods was counted, respectively. The results were shown in [Tab. 2](#). The results showed that the area of desertified land in the whole study area experienced a fluctuating trend of rapid increase and then a gradual decrease. Desertification in the study area, mild in all accounted for the largest percentage of desertified land, an average of 70%, followed by moderate desertification, and severe desertification and serious desertification, the proportion of smaller. 1989–2000 as the research area of desertification area rapid development stage, due to human factors such as grazing, grassland reclamation, desertification rapid deterioration. The total area increased from 458.73 km² in 1989 to 1559.95 km² in 2000, with an increase of 1101.22 km², and the area of desertification land of different degrees showed an obvious trend of expansion, among which the increase of mild desertification area was 698.36 km².

Table 2: Interdecadal variation of desertified land area in Gangcha Lake basin

Year		Mild desertification	Moderate desertification	Severe desertification	Serious desertification	Total
1989	area/km ²	341.84	66.34	33.32	17.23	458.73
	proportion/%	74.52	14.46	7.26	3.76	100.00
2000	area/km ²	1040.19	398.26	51.51	69.98	1559.95
	proportion/%	66.68	25.53	3.30	4.49	100.00
2009	area/km ²	983.17	375.14	28.15	27.65	1414.11
	proportion/%	69.53	26.53	1.99	1.96	100.00
2014	area/km ²	1020.41	254.25	51.07	44.49	1370.22

(Continued)

Table 2: Continued

Year		Mild desertification	Moderate desertification	Severe desertification	Serious desertification	Total
	proportion/%	74.47	18.56	3.73	3.25	100.00
Area of change /km ²	1989–2000	698.36	331.92	18.19	52.76	1101.22
	2000–2009	–57.02	–23.12	–23.36	–42.33	–145.84
	2009–2014	37.24	–120.89	22.91	16.84	–43.89

From 2000 to 2009, the total area of desertified land decreased by 145.84 km². This may be related to the formulation of regional desertification control policies, the active implementation of desertification control measures (sand fixation and grass planting, sand sealing and grassland breeding, returning farmland to grassland, rational grazing, etc.), and the enhancement of human environmental awareness. During this period, the area of different degrees of desertified land decreased, and the area of mild desertified land decreased the most, reaching 57.02 km². These changes show that the measures to control desertification in this period have achieved initial results.

From 2009 to 2014, the total area of desertified land in the study area was still decreasing, but the decreasing rate was significantly slower, and the total area of desertified land decreased only 43.89 km² during this period. However, according to the area change of different degree desertified land types, the area of moderate desertified land decreased significantly during this period, but the area of other degree desertified land increased. However, the overall trend is gradually improving, indicating that the ecological environment quality of the study area has been significantly improved.

5.2 Spatial Evolution of Desertified Land

According to the transfer matrix of desertified land of different grades in three periods (Tab. 3), it can be seen that during 1989–2000, the large area of non-desertified land was gradually desertified, which was mainly transformed into mild desertified land and moderate desertified land, with an area of 903.77 km² and 210.14 km² respectively. Only 14.13 km² and 29.88 km² were converted to severe desertification, respectively. The total area of desertified land reversed to non-desertified land was 62.54 km², which was much smaller than the total area of desertified land during this period (1157.92 km²), which indicated that the desertification situation was deteriorating in general during this period. During 1989–2000, mild desertified land was mainly degraded to moderate desertified land with an area of 165.52 km², followed by severely desertified land with an area of 20.32 km², and 5.80 km² to severely desertified land. Meanwhile, the area of mildly desertified land reversed to non-desertified land was 31.79 km². The area of moderate desertified land to severely desertified land was 10.40 km² and 11.06 km² respectively, and the area of moderate desertified land to mild desertified land and that of non-desertified land was 11.99 km² and 17.26 km² respectively. The area of severely desertified land was 8.39 km², and that of non-desertified land was 12.73 km². The area of mild desertified land was 5.38 km², and that of moderate desertified land was 3.25 km². The area of serious desertified land reversed to other land types was small.

Table 3: Desertification land transfer matrix of different degrees in the study area

Year	Land type	Mild desertification /km ²	Moderate desertification /km ²	Severe desertification /km ²	Serious desertification /km ²	No desertification /km ²	Total /km ²
1989~2000	Mild desertification	114.36	165.52	20.32	5.80	31.79	337.79
	Moderate desertification	11.99	13.83	10.40	11.06	17.26	64.54
	Severe desertification	5.38	3.25	2.75	8.39	12.73	32.49
	Serious desertification	1.73	2.97	2.06	9.03	0.67	16.48
	No desertification	903.77	210.14	14.73	29.88	1032.36	2190.88
	Total	1037.23	395.72	50.26	64.15	1094.82	2642.19
2000~2009	Mild desertification	693.30	112.57	1.90	2.44	229.47	1039.68
	Moderate desertification	139.06	226.21	11.45	4.37	16.47	397.56
	Severe desertification	13.72	17.85	9.56	3.80	6.11	51.03
	Serious desertification	31.87	10.86	4.71	15.24	3.92	66.59
	No desertification	97.86	6.14	0.26	0.37	991.46	1096.08
	Total	975.81	373.62	27.88	26.22	1247.41	2650.94
2009~2014	Mild desertification	685.30	57.69	9.20	4.87	212.98	970.02
	Moderate desertification	206.29	143.79	12.19	6.73	1.59	370.58
	Severe desertification	1.28	12.21	7.78	6.01	0.05	27.32
	Serious desertification	0.29	1.73	2.50	20.44	0.02	24.98
	No desertification	127.26	38.80	19.34	1.94	1023.63	1210.96
	Total	1020.41	254.21	51.00	39.99	1238.26	2603.87

From 2000 to 2009, the total area of non-desertified land converted to desertified land was 104.62 km², and the total area of desertified land converted to non-desertified land was 255.95 km², indicating that the trend of land change in this period was reverse desertification and the ecological status was getting better. The area of mild desertification land converted to moderate desertification land was 112.57 km², which was much larger than that of severe desertification land and severe desertification land. However, the area of moderate desertification land was 139.06 km², and the area of moderate desertification land was 139.06 km², and the area of moderate desertification land was 139.06 km². The area of severe desertification land was 13.72 km² and 17.85 km², respectively. The severe desertification land was mainly converted from

moderate desertification land, accounting for 62.5% of the total converted to severe desertification land. There was a distinct improvement in serious desertification land, into the largest proportion, mild desertified land conversion area of 31.87 km², followed by moderate desertification, 10.86 km², into the proportion of the severe desertification and desertification land types and smaller, similar serious desertification development is mainly by moderate desertification land conversion. It was 4.37 km², followed by severe desertification land and mild desertification land, and finally by non-desertification land, which was only 0.37 km².

From 2009 to 2014, the area of moderately desertified land decreased by 120.89 km², which was mainly reversed to mild desertified land (206.29 km²). Among the moderate desertified land types, mild desertified land accounted for 52%, followed by non-desertified land (35%). The area of mild desertified land was mainly reversed to non-desertified land, the area of mild desertified land was 57.69 km², the area of severely desertified land was 9.2 km² and the area of severely desertified land was 4.87 km². Severely desertified land was mainly converted from non-desertified land (19.34 km²), and moderate desertified land (12.19 km²), followed by severe desertified land (6.01 km²), developed land (19.34 km²) and moderate desertified land (12.19 km²). Severely desertification land was mainly converted from moderate desertification land and severe desertification land, and the area of serious desertification land was 6.73 km² and 6.01 km² respectively. The non-desertified land was mainly converted to mild desertified land (127.26 km²), followed by moderate desertified land (38.80 km²), and the increase of non-desertified land was mainly caused by the reversal of mild desertified land (212.98 km²). In general, desertification showed a slight reversal trend, and the variation trend was slightly different among different degrees of desertification, and desertification intensified in some areas.

5.3 Interannual Variation of Desertified Land Area

5.3.1 Characteristics of Annual Change of Desertified Land Area

Based on the classification results of remote sensing images, desertification information in the study area from 1988 to 2014 was extracted and statistically analyzed. For incomplete data in some years, linear interpolation method was used to complete the data, as shown in [Tab. 4](#).

Table 4: Extraction of desertification data in the study area

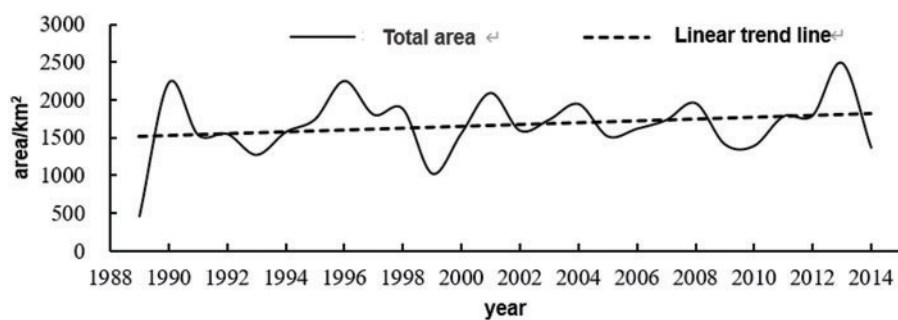
Year	Mild desertification /km ²	Moderate desertification /km ²	Severe desertification /km ²	Serious desertification /km ²	Total area of desertification/km ²
1989	341.84	66.34	33.32	17.23	458.73
1990	1550.73	619.49	36.83	23.06	2230.10
1991	988.16	463.25	52.88	35.69	1539.97
1992	989.64	470.52	55.75	36.30	1552.21
1993	1037.24	178.07	42.14	15.71	1273.16
1994	992.61	485.06	61.49	37.53	1576.69
1995	902.70	666.77	84.27	92.30	1746.05
1996	1259.86	915.32	56.94	22.80	2254.91
1997	1129.57	574.31	76.70	26.73	1807.32
1998	1099.74	711.29	51.46	21.46	1883.94

(Continued)

Table 4: Continued

Year	Mild desertification /km ²	Moderate desertification /km ²	Severe desertification /km ²	Serious desertification /km ²	Total area of desertification/km ²
1999	855.19	101.18	53.62	15.19	1025.17
2000	1040.19	398.26	51.51	69.98	1559.95
2001	758.65	885.66	299.09	152.81	2096.21
2002	1032.52	455.95	69.41	37.52	1595.39
2003	1004.07	642.04	59.01	35.94	1741.06
2004	1138.63	715.58	63.97	31.39	1949.56
2005	1107.66	353.78	28.01	29.88	1519.33
2006	756.22	743.77	82.84	37.78	1620.62
2007	1011.91	579.55	98.82	45.48	1735.77
2008	827.47	823.96	246.48	62.13	1960.03
2009	983.17	375.14	28.15	27.65	1414.11
2010	1046.54	259.99	62.29	24.11	1392.93
2011	1017.85	608.63	110.31	47.93	1784.71
2012	1019.33	615.90	113.18	48.54	1796.95
2013	1185.45	1064.87	189.23	55.39	2494.95
2014	1020.41	254.25	51.07	44.49	1370.22

As can be seen from the variation trend of the total area of desertified land in the study area (Fig. 4), the total area of desertified land increased year by year with an average change rate of 12.24 km²/y. The maximum area of desertified land was 2494.95 km² in 2013, and the minimum area was 458.73 km² in 1988. From 1989 to 2014, the total area of desertified land in the study area increased by 911.49 km², but its change trend was always in a state of fluctuation. This variation is influenced by climate, geographical location, human activities, and other factors, and is also closely related to the diversity of desertification.

**Figure 4:** Change characteristics of the total area of desertified land in the study area

As can be seen from the area changes of different grades of desertified land (Fig. 5), the main types of desertified land in the study area are mild and moderate desertification, and the proportion of severe and severe desertified land is small. However, the increasing rates were different. The increasing rates

of moderate desertification, severe desertification, mild desertification and severe desertification were $7.27 \text{ km}^2/\text{y}$, $2.87 \text{ km}^2/\text{y}$, $1.48 \text{ km}^2/\text{y}$ and $0.61 \text{ km}^2/\text{y}$, respectively. As shown in Fig. 5a, during 1989–1990, the area of mild desertification land increased sharply, with an increase of 1208.89 km^2 . After 1990, the area fluctuated steadily. The area of moderately desertified land showed obvious fluctuation, as shown in Fig. 5b. In 1989, 1993, 1999, 2010 and 2014, the area of moderately desertified land was small. During 1989–2014, the area of moderately desertified land increased by 187.91 km^2 . The area of severely desertified land showed a steady increase on the whole, and passed the significance test of 80% confidence, as shown in Fig. 5c. The area of severely desertified land expanded rapidly in 2001, 2008 and 2013, and increased by 17.74 km^2 from 1989 to 2014. The area of severely desertified land changed gently, as shown in Fig. 5d. The expansion rate in 1995 and 2001 was significant, and the area of severely desertified land increased by 27.26 km^2 from 1989 to 2014. In general, the increase of desertified land area of different degrees aggravated desertification in the study area.

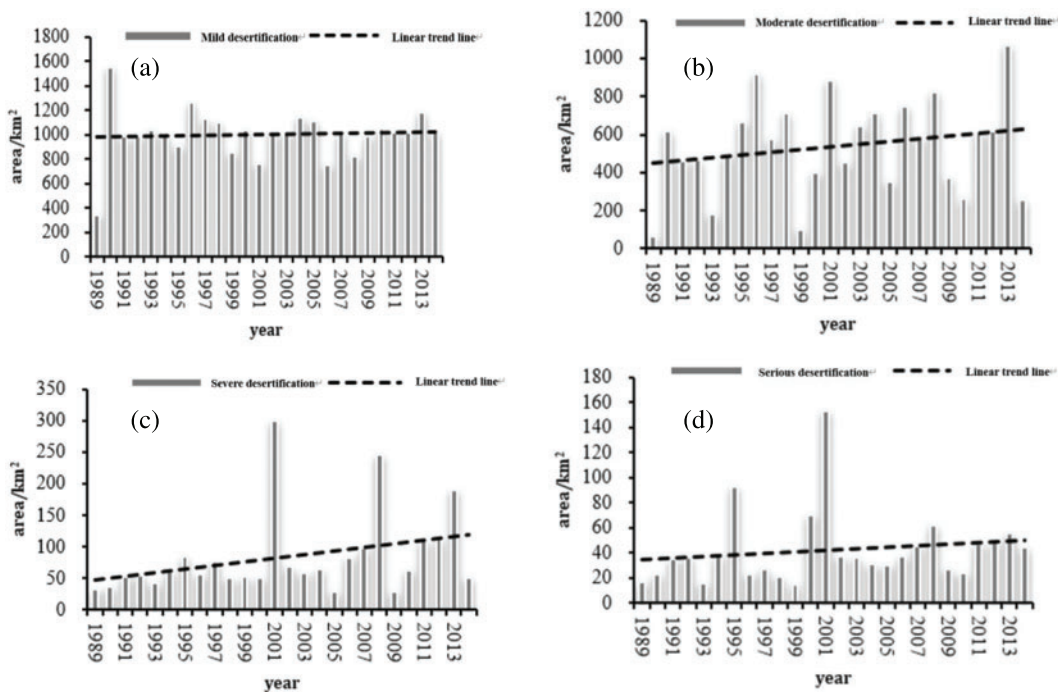


Figure 5: The interannual variation characteristics of different degrees of desertification land area in the study area: (a) Mild desertification; (b) Moderate desertification; (c) Severe desertification; (d) Serious desertification

5.3.2 Characteristics of Annual Change of Area Increment of Desertified Land

The increment of the desertified land area can well reflect the change amplitude and trend of desertified land area. The increment information of different types of desertified land area in the study area from 1990 to 2014 is shown in Tab. 5.

Table 5: Desertification land transfer matrix of different degrees in the study area

Year	Mild desertification increment /km ²	Moderate desertification increment /km ²	Severe desertification increment /km ²	Serious desertification increment /km ²	Total area of desertification /km ²
1990	1208.89	553.15	3.50	5.84	1771.38
1991	-562.57	-156.24	16.05	12.63	-690.13
1992	1.48	7.27	2.87	0.61	12.24
1993	47.60	-292.45	-13.61	-20.59	-279.05
1994	-44.63	306.98	19.35	21.82	303.52
1995	-89.91	181.72	22.78	54.78	169.37
1996	357.16	248.54	-27.33	-69.51	508.86
1997	-130.30	-341.00	19.76	3.94	-447.60
1998	-29.83	136.97	-25.25	-5.28	76.62
1999	-244.55	-610.11	2.16	-6.27	-858.77
2000	185.00	297.08	-2.10	54.80	534.78
2001	-281.55	487.40	247.57	82.83	536.26
2002	273.87	-429.71	-229.68	-115.29	-500.81
2003	-28.45	186.09	-10.40	-1.58	145.67
2004	134.55	73.54	4.96	-4.55	208.50
2005	-30.97	-361.80	-35.96	-1.51	-430.24
2006	-351.44	389.99	54.84	7.90	101.29
2007	255.69	-164.22	15.98	7.70	115.15
2008	-184.44	244.41	147.65	16.65	224.27
2009	155.71	-448.82	-218.33	-34.48	-545.92
2010	63.36	-115.14	34.14	-3.55	-21.18
2011	-28.69	348.63	48.02	23.82	391.79
2012	1.48	7.27	2.87	0.61	12.24
2013	166.12	448.98	76.05	6.85	698.00
2014	-165.04	-810.63	-138.16	-10.90	-1124.73

In general, the increment of the total area of desertification in the study area showed a decreasing trend year by year (Fig. 6) with a decreasing rate of $-15.08 \text{ km}^2/\text{y}$, while the total area of desertification in the study area showed an increasing trend, indicating that the increase rate of the total area of desertification was gradually slowing down. The increment of the total area of desertification in the study area was the largest in 1990, with an area increase value of 1771.38 km^2 , indicating that desertification in the study area deteriorated sharply in 1990, while the minimum increment value was -1124.73 km^2 in 2014, indicating that desertification in the study area improved significantly in 2014.

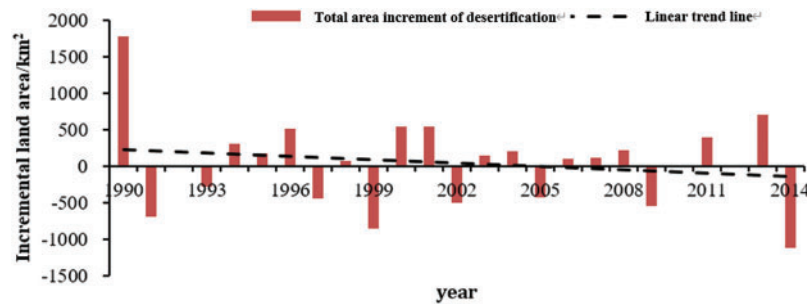


Figure 6: Interannual variation of the increment of the total area of desertification

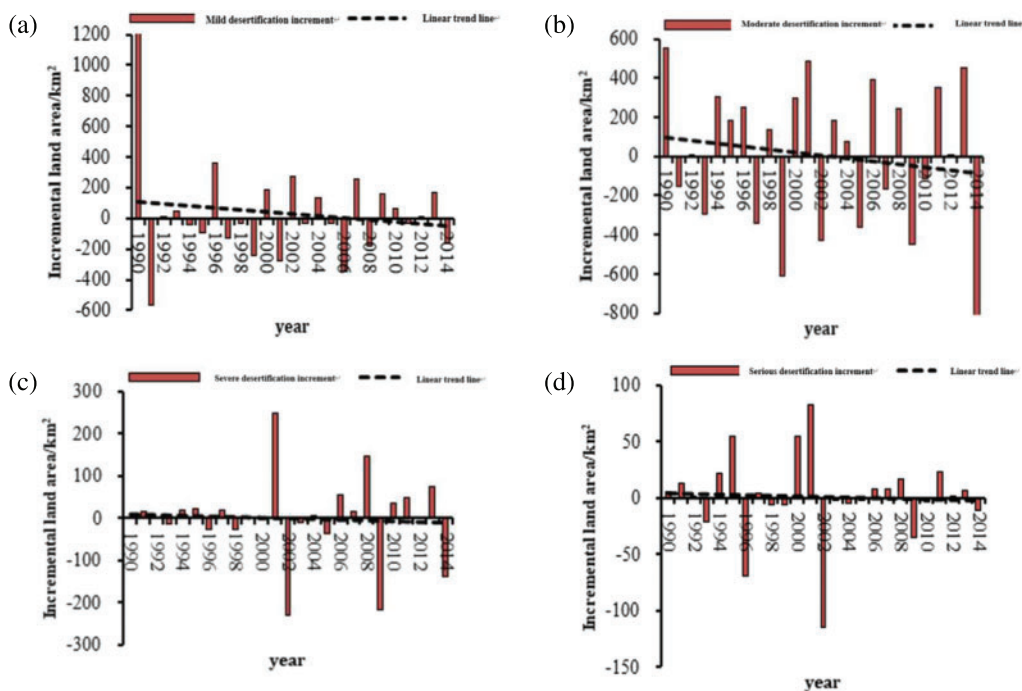


Figure 7: The interannual variation characteristics of land area increment of different desertification types in the study area : (a) mild desertification increment; (b) Moderate desertification increment; (c) Severe desertification increment; (d) Serious desertification increment

As shown in Fig. 7, the different types of desertified land area in the study area increment all showed a trend of decrease in the time series, but decrease rate differences of different types of desertified land area, its absolute value from big to small, in the desertification of moderate desertification increment, the increment, the severe desertification increment, severe desertification increment, The change rates were $-7.59 \text{ km}^2/\text{y}$, $-6.45 \text{ km}^2/\text{y}$, $-0.82 \text{ km}^2/\text{y}$ and $-0.23 \text{ km}^2/\text{y}$, respectively. The previous results showed that the area of different types of desertified land was increasing year by year, indicating that the increasing trend of different types of desertified land was gradually slowing down and desertification was improving. As shown in Fig. 7a, the maximum increment of mild desertification occurred in 1990, with an increment of 1208.89 km^2 , while the minimum increment occurred in 1991, with an increment of -562.57 km^2 . As shown in Fig. 7b, the increment of moderate desertification land area showed significant fluctuation. Desertification change increased and decreased during this

period. The maximum value of moderate desertification increment appeared in 1990 with an increment of 553.15 km^2 , while the minimum value appeared in 2014 with an increment of -810.63 km^2 . As shown in Fig. 7c, the change of moderate desertification increment was moderate before 2000. In 2001, the maximum value of severe desertification increment was 247.57 km^2 , followed by the minimum value of -229.68 km^2 in 2002. After 2002, the increment change amplitude increased significantly. As shown in Fig. 7d, the maximum increment of serious desertification land area appeared in 2001, which was 82.83 km^2 , while the minimum increment appeared in 2002, which was -115.29 km^2 . In conclusion, the abrupt change points of mild and moderate desertification land area increment were located in 1990 and 2014, while the abrupt change points of severe and severe desertification land area increment were located in 2001 and 2002.

6 Conclusion

In this study, the lake basin area of Gangcha County as the study area was used to analysis the trend of desertification. The multi-phase remote sensing image of the study area was interpreted by RS technology, and the desertification land information of the study area in the past 26 years was extracted. The Desertified land in the area is divided into four grades: light desertification, moderate desertification, heavy desertification, and severe desertification by decision tree classification and statistics on the area and spatial distribution of different degrees of desertification land in the study area. The results of desertification data analysis show that since 1989, the overall desertification in the study area has experienced a fluctuating process of first deterioration and then improvement. The 1990s was the stage of rapid development of desertification in the study area. During this period, the total area of desertification increased by 1101.22 km^2 . The land area has shown a significant increase trend, of which the lightly desertified land has the largest increase, and the expansion area has reached 698.36 km^2 . Since the 21st century, the overall desertification in the study area has shown a gradual improvement trend, but local desertification is still aggravating. Through the analysis of the data of the desertified land in the study area over the years, it is found that the total area of desertification in the study area showed a significant increase from 1989 to 2014, with an increased rate of $12.24\text{ km}^2/\text{y}$. The area of desertification land in different degrees has an increasing trend, but the increase rate is different. Among them, the area of moderately desertified land has the largest spread rate, which is $+7.27\text{ km}^2/\text{y}$; followed by heavily desertified land and lightly desertified land, with rates of $+2.87\text{ km}^2/\text{y}$ and $1.48\text{ km}^2/\text{y}$, the change rate of the severely desertified land area is the smallest, which is $+0.61\text{ km}^2/\text{y}$. The increase in the area of different types of desertification showed a downward trend, indicating that the increase in the area of desertification in the study area was slowing down. In 1990 and 2002, the increase in desertification was generally large, and there was an obvious mutation effect.

Acknowledgement: This work was supported by the National Natural Science Foundation of China “Study on the dynamic mechanism of grassland ecosystem response to climate change in Qinghai Plateau” under grant number U20A2098.

Funding Statement: This work was supported by the National Natural Science Foundation of China “Study on the dynamic mechanism of grassland ecosystem response to climate change in Qinghai Plateau” under grant number U20A2098.

Conflicts of Interest: The authors declare that they have no conflicts of interest to report regarding the present study.

References

- [1] L. L. Lavauden, *Forêts du Sahara*. Paris, France, Impr. Berger-Levrault, 1927.
- [2] M. M. Verstraete, "Defining desertification: A review," *Climatic Change*, vol. 9, no. 1–2, pp. 5–18, 1986.
- [3] Z. D. Zhu, S. Liu and Z. Wu, *An introduction to Deserts in China*. Beijing, China, Science Press, 1980.
- [4] N. P. Hanan, Y. Prevost and A. Diouf, "Assessment of desertification around deep wells in the Sahel using satellite imagery," *Journal of Applied Ecology*, vol. 28, no. 1, pp. 173–186, 1991.
- [5] G. K. Tripathy, T. K. Ghosh and S. D. Shah, "Monitoring of desertification process in Karnataka state of India using multi-temporal remote sensing and ancillary information using GIS," *International Journal of Remote Sensing*, vol. 17, no. 12, pp. 2243–2257, 1996.
- [6] B. Nasem and G. Rudi, "A satellite-based disturbance index algorithm for monitoring mitigation strategies effects on desertification change in an arid environment," *Mitigation and Adaptation Strategies for Global Change*, vol. 20, no. 2, pp. 263–276, 2015.
- [7] W. Wu, "Methods and practice of desertification dynamic monitoring by remote sensing," *Remote Sensing Technology and Application*, vol. 12, no. 4, pp. 14–20, 1997.
- [8] W. Wu, "Dynamic monitor to evolvement of sandy desertified Land in horqin region for the Last 5 decades, China," *Journal of Desert Research*, vol. 23, no. 6, pp. 646–651, 2003.
- [9] H. W. Li and X. P. Yang, "Advances and problems in the understanding of desertification in the hunshandake sandy land during the last 30 years," *Advances in Earth Science*, vol. 25, no. 6, pp. 647–655, 2010.
- [10] G. Y. Hu, Z. B. Dong and J. F. Lu, "Spatial and temporal changes of desertification land and its influence factors in source region of the yellow river from 1975 to 2005," *Journal of Desert Research*, vol. 31, no. 5, pp. 1079–1086, 2011.
- [11] G. Y. Hu, Z. B. Dong and J. F. Lu, "Desertification and change of landscape pattern in the Source Region of Yellow River," *Acta Ecologica Sinica*, vol. 31, no. 14, pp. 3872–3881, 2011.
- [12] Y. X. Dong, "Progresses and problems in research on sandy desertification in Qinghai-Xizang plateau," *Journal of Desert Research*, vol. 19, no. 3, pp. 251–255, 1999.
- [13] S. Li, Y. X. Dong and G. R. Dong, "Regionalization of land desertification on Qinghai-Tebet plateau," *Journal of Desert Research*, vol. 21, no. 4, pp. 418–427, 2001.
- [14] Y. S. Zhao, *Principle and method of remote sensing application analysis*. Beijing, China, Science Press, 2003.
- [15] S. H. Tang, "A simple method to estimate crown cover fraction and rebuild the background information," *Journal of Image and Graphics*, vol. 8, no. 11, pp. 1309–1340, 2003.
- [16] M. M. Li, "Estimation of vegetation fraction in the upper basin of Miyun reservoir by remote sensing," *Resources Science*, vol. 26, no. 4, pp. 157–164, 2004.
- [17] C. Leprieur, M. M. Verstraete and B. Pinty, "Evaluation of the performance of various vegetation indices to retrieve vegetation cover from AVHRR data," *Remote Sensing Review*, vol. 10, no. 4, pp. 265–284, 1994.
- [18] C. R. Bradley, "The influence of canopy green vegetation fraction on spectral measurements over native tall grass prairie," *Remote Sensing of Environment*, vol. 81, no. 1, pp. 129–135, 2002.
- [19] J. G. Qi, A. R. Chehbouni and A. R. Huete, "A modified soil adjusted vegetation index," *Remote sensing of Environment*, vol. 48, no. 2, pp. 119–126, 1994.
- [20] Z. H. Qin, "Mono-window algorithm for retrieving land surface temperature from landsat TM6 data," *Acta Geographica Sinica*, vol. 56, no. 4, pp. 456–466, 2001.
- [21] I. Sandholt, K. Rasmussen and J. Andersen, "A simple interpretation of the surface temperature/vegetation index space for assessment of surface moisture status," *Remote Sensing of Environment*, vol. 79, no. 2-3, pp. 213–224, 2002.
- [22] M. Story and R. G. Congalton, "Accuracy assessment: A user's perspective," *Photogrammetric Engineering & Remote Sensing*, vol. 48, no. 1, pp. 131–137, 1986.
- [23] I. F. J. Lucas and J. M. Fransand, "Accuracy assessment of satellite derived land-cover data: A review," *Photogrammetric Engineering & Remote Sensing*, vol. 60, no. 4, pp. 410–432, 1994.

- [24] Q. He, S. Yu, H. Xu, J. Liu, D. Huang *et al.*, “A weighted threshold secret sharing scheme for remote sensing images based on chinese remainder theorem,” *Computers Materials & Continua*, vol. 58, no. 2, pp. 349–361, 2019.
- [25] C. Srinivas and K. C. Rao, “Adaptive signal enhancement unit for eeg analysis in remote patient care monitoring systems,” *Computers Materials & Continua*, vol. 67, no. 2, pp. 1801–1817, 2021.
- [26] M. M. Alshahrani, “Secure multifactor remote access user authentication framework for iot networks,” *Computers Materials & Continua*, vol. 68, no. 3, pp. 3235–3254, 2021.
- [27] W. Sung and S. Hsiao, “Rfid positioning and physiological signals for remote medical care,” *Computer Systems Science and Engineering*, vol. 41, no. 1, pp. 289–304, 2022.
- [28] H. Kwon, S. Hong, M. Kang and J. Seo, “Data traffic reduction with compressed sensing in an aiot system,” *Computers Materials & Continua*, vol. 70, no. 1, pp. 1769–1780, 2022.